

---

# ACCELERATING ODE-BASED NEURAL NETWORKS ON LOW-COST FPGAs

---

A PREPRINT

**Hirohisa Watanabe**

Keio University  
3-14-1 Hiyoshi, Kohoku-ku, Yokohama, Japan  
watanabe@arc.ics.keio.ac.jp

**Hiroki Matsutani**

Keio University  
3-14-1 Hiyoshi, Kohoku-ku, Yokohama, Japan  
matutani@arc.ics.keio.ac.jp

January 5, 2021

## ABSTRACT

ODENet is a deep neural network architecture in which a stacking structure of ResNet is implemented with an ordinary differential equation (ODE) solver. It can reduce the number of parameters and strike a balance between accuracy and performance by selecting a proper solver. It is also possible to improve the accuracy while keeping the same number of parameters on resource-limited edge devices. In this paper, using Euler method as an ODE solver, a part of ODENet is implemented as a dedicated logic on a low-cost FPGA (Field-Programmable Gate Array) board, such as PYNQ-Z2 board. Two variants, one for high accuracy and the other for performance, are proposed and implemented on the FPGA board as well. They are evaluated in terms of parameter size, accuracy, execution time, and resource utilization on the FPGA. The results show that an overall execution time of ODENet and its variants is improved by up to 2.50 times compared to a pure software execution when a part of convolution layers is executed by the programmable logic.

**Keywords** Neural network · ODE · Neural ODE · FPGA

## 1 Introduction

ResNet [1] is a well-known deep neural network architecture with high accuracy. In addition to conventional forward propagation of deep neural networks, it has shortcut or skip connections that directly add the input of a layer to the output of the layer. Since it can mitigate vanishing and exploding gradient problems, we can stack more layers to improve prediction accuracy. However, stacking many layers increases the number of parameters of deep neural networks; in this case, memory requirement becomes severe in resource-limited edge devices.

ODENet [2] that employs an ordinary differential equation (ODE) solver in deep neural networks was proposed to reduce weight parameters of the network. Stacking structure of layers in ResNet can be represented with an ODE solver, such as Euler method. ODENet thus uses an ODE solver in prediction and training processes so that  $M$  layers in ResNet are replaced with  $M$  repeated executions of a single layer, as shown in Figures 1 and 2. In this case, ODENet can significantly reduce the number of parameters compared to the original ResNet while keeping the equivalent prediction and training processes.

Field-Programmable Gate Array (FPGA) is an energy-efficient solution, and it has been widely used in edge devices for machine learning applications [3]. In this paper, we thus propose an FPGA-based acceleration of ODENet. A core component of ODENet, called ODEBlock, that consists of convolution layers, batch normalization [4], and activation function is implemented on a programmable logic of low-cost FPGA board, such as PYNQ-Z2 board. Its two variant implementations, one for high accuracy and the other for performance, are also proposed. They are evaluated in terms of parameter size, accuracy, execution time, and resource utilization on the FPGA.

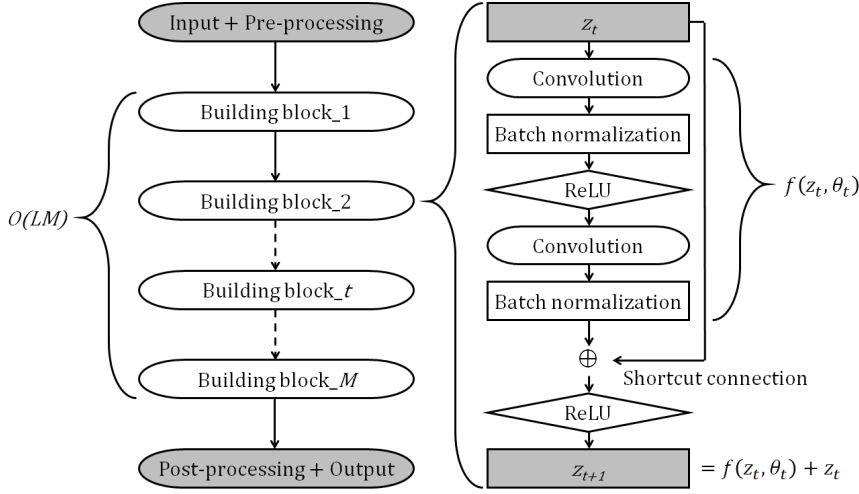


Figure 1: ResNet architecture

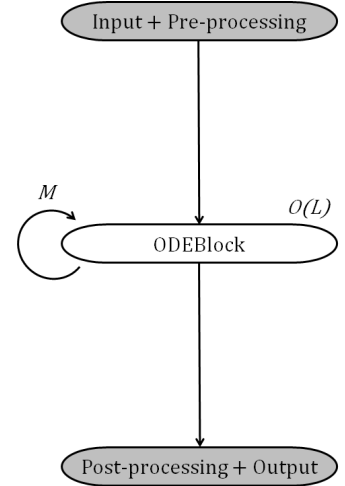


Figure 2: ODENet architecture

The rest of this paper is organized as follows. Section 2 provides a brief review of basic technologies about ODENet. Section 3 implements a building block of ODENet on the FPGA, and Section 4 shows the evaluation results. Section 5 concludes this paper.

## 2 Preliminaries

### 2.1 ResNet

In neural networks that serially stack many layers, training process may be prevented when gradients become vanishingly small in one of the layers (i.e., vanishing gradient problem). Also, there may be possibility that the training becomes unstable when gradient descent is diverging (i.e., exploding gradient problem). ResNet [1] was proposed to address these issues and improve the prediction accuracy by introducing shortcut connections that enable to stack many layers. Figure 1 illustrates ResNet architecture. As shown in the figure, ResNet consists of a lot of building blocks. Each building block receives input data  $z_t$  and executes  $3 \times 3$  convolution, batch normalization [4], ReLU [5] as an activation function,  $3 \times 3$  convolution, and batch normalization. For example, ResNet architecture, which will be shown in Table 2, can be used in image classification tasks, such as CIFAR-10 and CIFAR-100 datasets. In this paper, building blocks executing the same computations are grouped as layer  $x$ , where  $x = 1, 2, 3$ . ResNet size is denoted as ResNet-N, where N is the total number of convolution steps in the building blocks including the pre- and post-processing layers.

Let  $z \in \mathbb{R}^Z$  and  $y \in \mathbb{R}^Z$  be an input and an output of ResNet, respectively. A network parameter  $\theta$  is interpreted as a mapping function  $\mathcal{H} : z \rightarrow y$ . Assuming a normal forward propagation, an output of a building block is represented as a function  $f(z, \theta)$ . When an input of a building block is additionally added to an output of the building block with a shortcut connection, the function is changed to  $f(z, \theta) + z$ . Even with a shortcut connection, an output of the building block itself is still  $\mathcal{H}(z)$ . Thus, its residual should be trained in the training process so that  $f(z, \theta) = \mathcal{H}(z) - z$ . In this case, a gradient at least contains 1; thus, vanishing gradient problem can be mitigated.

Assuming ResNet consists of multiple building blocks, an input to the  $(t + 1)$ -th building block is represented as follows.

$$z_{t+1} = z_t + f(z_t, \theta_t), \quad (1)$$

where  $z_t$  and  $\theta_t$  denote the input and parameter of the  $t$ -th building block, respectively.

### 2.2 Ordinary Differential Equation

ODE is an equation containing functions of one variable and their derivatives. For example, a first-order differential equation is represented as follows.

$$\frac{dz}{dt} = f(z(t), t, \theta), \quad (2)$$

where  $f$  and  $\theta$  represent dynamics and the other parameters, respectively. Assuming  $f$  is known and  $z(t_0)$  is given, a problem to find  $z(t_1)$  that satisfies the above equation is known as an initial value problem. It is formulated as follows.

$$z(t_1) = z(t_0) + \int_{t_0}^{t_1} f(z(t), t, \theta) dt \quad (3)$$

$$= \text{ODESolve}(z(t_0), t_0, t_1, f) \quad (4)$$

In the right side of Equation 3, the second term contains an integral of a given function. It cannot be solved analytically for arbitrary functions, so a numerical approximation is typically employed to solve Equation 3. To solve the equation, ODESolve function is defined as shown in Equation 4. In ODESolve function, integration range  $[t_0, t_1]$  is divided into partitions with step size  $h$ . For  $t_0 < \dots < t_i < \dots < t_1$ , it computes corresponding  $z_i$  using a recurrence formula. As a method to compute  $z(t_1)$  in Equation 4, well-known ODE solvers, such as Euler method, second-order Runge-Kutta method, and fourth-order Runge-Kutta method, can be used [6]. They can approximately solve Equation 3 in the first-order, second-order, and fourth-order accuracy, respectively. Below is Euler method.

$$z(t_{i+1}) = z(t_i) + hf(z(t_i), t_i, \theta) \quad (5)$$

### 2.3 ODENet

An output of building blocks in ResNet can be computed with a recurrence formula, as shown in Equation 1. Please note that Equation 1 is similar to Equation 5 except that the former basically assumes vector values while the latter assumes scalar values. Thus, one building block is interpreted as one step in Euler method. As mentioned in Section 2.2, since Euler method is a first-order approximation of Equation 3, an output of ResNet can be interpreted as well. Since Equation 3 can be solved by Equation 4, the output of ResNet can be solved by the same equation. Here, a building block of ResNet is replaced with an ODEBlock using ODESolve function. Neural network architecture consisting of such ODEBlocks is called ODENet. Figure 2 shows an ODENet architecture. ODENet that repeats the same ODEBlock  $M$  times is interpreted as ResNet with  $M$  building blocks.

Prediction tasks of ODENet are executed based on Equation 4. In training process, it is required that gradients are back-propagated along neural network layers via ODESolve function. To compute the gradients, ODENet uses an adjoint method [7] in the training process. Here, loss function  $L$  of ODENet is represented as follows.

$$L(z(t_1)) = L(\text{ODESolve}(z(t_0), t_0, t_1, f)) \quad (6)$$

Let an adjoint vector  $\mathbf{a}$  be  $\mathbf{a} = \frac{\partial L}{\partial \mathbf{z}(t)}$ . The following equation is satisfied with respect to  $\mathbf{a}$ .

$$\frac{d\mathbf{a}(t)}{dt} = -\mathbf{a}^\top \frac{\partial f(\mathbf{z}(t), t, \theta)}{\partial \mathbf{z}(t)} \quad (7)$$

Based on Equations 7 and 4, a gradient of parameter  $\theta$  derived by a loss function is computed as follows.

$$\begin{aligned} \frac{dL}{d\theta} &= - \int_{t_1}^{t_0} \mathbf{a}(t)^\top \frac{\partial f(\mathbf{z}(t), t, \theta)}{\partial \theta} dt \\ &= \text{ODESolve} \left( \mathbf{0}, t_1, t_0, -\mathbf{a}(t)^\top \frac{\partial f(\mathbf{z}(t), t, \theta)}{\partial \theta} \right) \end{aligned} \quad (8)$$

$\mathbf{z}(t)$  and  $\mathbf{a}(t)$  can be computed with ODESolve function. A training function can be summarized as follows by using Equation 8 and these values.

$$\begin{aligned} \mathbf{z}(t_0) &= \text{ODESolve}(\mathbf{z}(t_1), t_1, t_0, f(\mathbf{z}(t), t, \theta)) \\ \mathbf{a}(t_0) &= \text{ODESolve} \left( \mathbf{a}(t_1), t_1, t_0, -\mathbf{a}(t)^\top \frac{\partial f(\mathbf{z}(t), t, \theta)}{\partial \mathbf{z}(t)} \right) \\ \frac{dL}{d\theta} &= \text{ODESolve} \left( \mathbf{0}, t_1, t_0, -\mathbf{a}(t)^\top \frac{\partial f(\mathbf{z}(t), t, \theta)}{\partial \theta} \right) \end{aligned} \quad (9)$$

Please note that vector size of  $\mathbf{0}$  in Equation 9 is same as that of  $\theta$ . In the original Equation 8, it is necessary to compute  $\mathbf{a}(t)$  and  $\mathbf{z}(t)$  for each  $t$ . On the other hand, in the case of Equation 9,  $\mathbf{z}(t)$  is computed first using ODESolve function; then  $\mathbf{a}(t)$  is computed based on  $\mathbf{z}(t)$ , and the gradient is computed based on  $\mathbf{z}(t)$  and  $\mathbf{a}(t)$ . Thus, the gradient is computed sequentially without keeping  $\mathbf{a}(t)$  and  $\mathbf{z}(t)$  for each  $t$ , so memory usage can be reduced as well. Based on the above-mentioned properties of ODENet, the benefit against the original ResNet is that the number of parameters can be reduced by ODENet. In the prediction process, ResNet is represented with  $M$  different building blocks, while

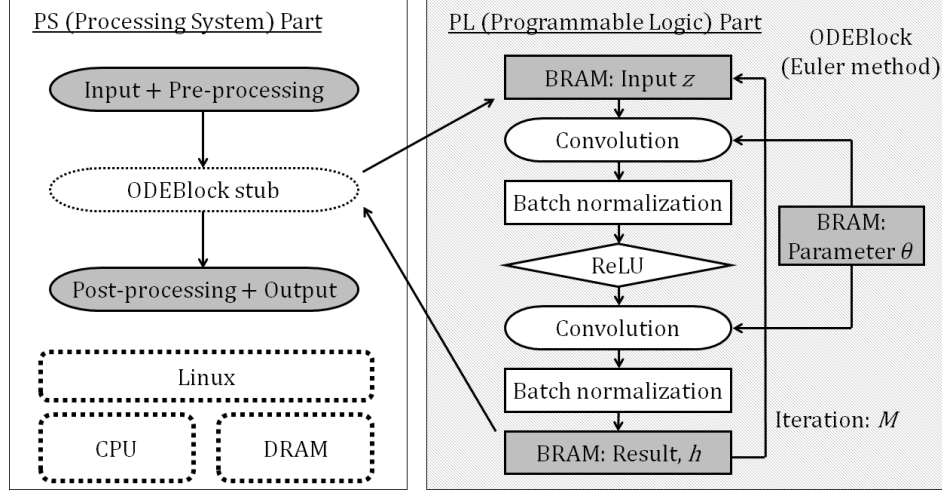


Figure 3: ODEBlock design on FPGA

ODENet repeatedly uses a single ODEBlock  $M$  times. When the number of parameters for one building block is  $O(L)$ , those of ResNet and ODENet are  $O(LM)$  and  $O(L)$ , respectively. Typically, the number of parameters for pre- and post-processing layers is not significant, it is expected that the number of parameters of ResNet is reduced to approximately  $\frac{1}{M}$ . In other words, in Equation 1, different parameters are used for each  $t$ . In ODENet, on the other hand, as shown in Equation 2,  $\theta$  is independent of  $t$ ; thus, it can be trained while the parameters are fixed irrespective of  $t$ . Please note that different ODE solvers can be used in prediction and training processes. For example, a fourth-order Runge-Kutta method is used for training with high accuracy, while Euler method is used for prediction tasks for low latency and simplicity. We can strike a balance between accuracy and performance by selecting a proper solver.

### 3 FPGA Implementation

In this paper, as a target platform, we employ SoC type FPGA devices that integrate programmable logic (PL) part and processor (PS) part, as shown in Figure 3. PS part consists of CPU and DRAM, while PL part has programmable logic. We use TUL PYNQ-Z2 board in this paper [8]. Figure 4 shows the FPGA board, and Table 1 shows the specification. As shown in Figure 3, a part of ODEBlock is implemented on PL part as a dedicated circuit, while the others are executed on PS part as software. Although PS and PL parts are typically connected via AXI bus and DMA transfer is used for their communication as in [3], the communication interface has not been implemented yet.

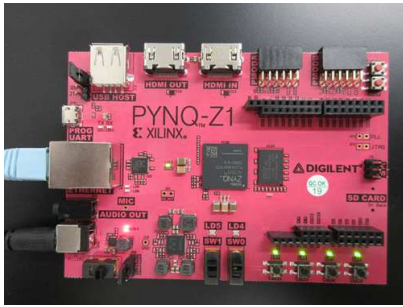


Table 1: Specification of PYNQ-Z2 board

OS	PYNQ Linux (Ubuntu 18.04)
CPU	ARM Cortex-A9 @ 650MHz $\times$ 2
DRAM	512MB (DDR3)
FPGA	Xilinx Zynq XC7Z020-1CLG400C

Figure 4: Overview of PYNQ-Z2 board

Table 2 shows network structure of ResNet, ODENet, and variants. They consist of several building blocks or “layers” as shown in the table. Among these layers, the number of parameters in layer3\_2 is the smallest; thus, layer3\_2 is implemented on a resource-limited FPGA board in this paper. More specifically, layer3\_2 is implemented on PL part of PYNQ-Z2, while the other parts are executed on PS part as software. Euler method is used as an ODE solver.

layer3\_2 consists of five steps: 1) convolution (input/output channel number: 64, input/output feature map:  $8 \times 8$ , kernel size:  $3 \times 3$ , and stride: 1), 2) batch normalization, 3) activation function (ReLU), 4) convolution, and 5) batch normalization. The above mentioned five steps are implemented in Verilog HDL. 32-bit Q20 fixed-point number

format is used. Multiply-add units are used in the convolution and ReLU steps, and multiply-add units, division unit, and square root unit are used in the batch normalization steps to compute mean, variance, and standard deviation. Weight parameters  $\theta$  of the two convolution steps are stored in Block RAM (BRAM) of the FPGA. Input and output feature maps for all the channels are also stored in BRAM.

Most of computation time is consumed in the convolution steps<sup>1</sup>. Our convolution and ReLU step implementations are scalable; that is, we can increase the number of multiply-add units from 1 to 64 depending on available resources. Their execution cycles (except for the batch normalization) decrease in inverse proportion to the number of multiply-add units. We implemented layer3\_2 with 1, 4, 8, 16, and 32 multiply-add units. They are referred to as conv\_x1, conv\_x4, conv\_x8, conv\_x16, and conv\_x32, respectively. Their execution cycles of layer3\_2 are 23.78M, 6.07M, 3.12M, 1.64M, and 0.90M cycles, respectively. In these implementations, since only conv\_x32 could not satisfy a timing constraint of our target FPGA board (i.e., 100MHz), we mainly use conv\_x16 in this paper.

## 4 Evaluations

CIFAR-100 is used as a dataset in this paper. ODENet on the FPGA is evaluated in terms of the number of parameters, accuracy, execution time, and resource utilization of the FPGA.

### 4.1 Network Configuration

As shown in Table 2, four network architectures listed below are used in this evaluation. Please note that the number of block stackings means the number of block instances implemented, while the number of block executions means the number of iterations on the same block instance.

- **ResNet-N**: Baseline ResNet
- **ODENet-N**: layer2\_2 and layer3\_2 in **ResNet-N** are replaced with ODEBlock. layer3\_2 is implemented on PL part of the FPGA.
- **Mixed-ODENet-N**: Only layer3\_2 in **ResNet-N** is replaced with ODEBlock. layer3\_2 is implemented on PL part of the FPGA.
- **Biased-ODENet-N**: Only a single building block is stacked for layer1 in **ResNet-N**. In addition, layer2\_2 is removed and the number of executions on layer3\_2 is increased instead, because layer3\_2 is implemented on PL part of the FPGA. As a result, total execution count of building blocks is same as the other architectures.

**ODENet-N** and **Mixed-ODENet-N** execute the same computation as **ResNet-N**. **Biased-ODENet-N** executes the same number of building blocks as **ResNet-N**, but it heavily uses layer3\_2 so that execution on PL part in Figure 3 is increased.

Euler method is used as an ODE solver, because it is simple and requires only a small temporary memory at prediction time. In Table 2, conv1 is the pre-processing step that executes  $3 \times 3$  convolution, batch normalization, and activation function ReLU. Then, various building blocks (e.g., layer1 to layer3\_2 in Table 2) are executed as shown in Figure 1. Finally, fc is the post-processing step that executes global average pooling, fully connected layer to all the output classes, and activation function Softmax. Stride width is set to 1 in most of building blocks except for layer2\_1 and layer3\_1, in which stride width is set to 2 in order to reduce the output feature map.

### 4.2 Parameter Size

Table 3 shows the total parameter size for each architecture listed in Section 4.1, assuming that each parameter is implemented in a 32-bit format.

- As shown in Table 3, parameter size of **ResNet-N** is proportional to the number of stacked building blocks (see Table 2).
- Please note that parameter sizes of **ODENet-N** and **Biased-ODENet** are independent of N. The difference on their parameter sizes comes only from layer2\_2. When N is 20 (the smallest case), parameter sizes of **ODENet-N** and **Biased-ODENet** are 36.24% and 43.29% less than that of **ResNet-20**, respectively. When N is 56 (the largest case), their parameter sizes are 79.55% and 81.80% less than that of **ResNet-20**, respectively.

<sup>1</sup>The two convolution steps consume about 99% of execution cycles of layer3\_2 when only a single multiply-add unit is used in our implementation.

Table 2: Network structure of ResNet, ODENet, and variants

Layer	Output size	Detail	Numbers of block stacking / execution			
			ResNet-N	ODENet-N	Mixed-ODENet-N	Biased-ODENet-N
conv1	$32 \times 32$ , 16ch	$3 \times 3$ , stride 1	1 / 1	1 / 1	1 / 1	1 / 1
layer1	$32 \times 32$ , 16ch	$\begin{smallmatrix} 3 \times 3 \\ 3 \times 3 \end{smallmatrix}$ , stride 1	$\frac{N-2}{6} / 1$	$1 / \frac{N-2}{6}$	$\frac{N-2}{6} / 1$	1 / 1
layer2_1	$16 \times 16$ , 32ch	$\begin{smallmatrix} 3 \times 3 \\ 3 \times 3 \end{smallmatrix}$ , stride 2	1 / 1	1 / 1	1 / 1	1 / 1
layer2_2	$16 \times 16$ , 32ch	$\begin{smallmatrix} 3 \times 3 \\ 3 \times 3 \end{smallmatrix}$ , stride 1	$\frac{N-2}{6} - 1 / 1$	$1 / \frac{N-2}{6} - 1$	$\frac{N-2}{6} - 1 / 1$	0 / 0
layer3_1	$8 \times 8$ , 64ch	$\begin{smallmatrix} 3 \times 3 \\ 3 \times 3 \end{smallmatrix}$ , stride 2	1 / 1	1 / 1	1 / 1	1 / 1
layer3_2	$8 \times 8$ , 64ch	$\begin{smallmatrix} 3 \times 3 \\ 3 \times 3 \end{smallmatrix}$ , stride 1	$\frac{N-2}{6} - 1 / 1$	$1 / \frac{N-2}{6} - 1$	$1 / \frac{N-2}{6} - 1$	$1 / \frac{N-8}{2}$
fc	$1 \times 100$	Average pooling, 100-d fc, softmax	1 / 1	1 / 1	1 / 1	1 / 1

- Although structure of **Mixed-ODENet-N** is similar to that of **ResNet-N** except for layer3\_2, it can reduce the parameter size by 26.42% and 60.16% compared to **ResNet-N** when N is 20 and 56, respectively.

As shown, using ODEBlock can reduce the parameter size compared to **ResNet-N**. **Biased-ODENet-N** is the smallest, followed in order by **ODENet-N** and **Mixed-ODENet-N**. The parameter size reduction becomes large as N is increased. Because parameter size reduction by using ODEBlock is independent of the other parameter reduction techniques, it can incorporate DNN quantization methods to further reduce the parameter size.

Table 3: Parameter size of ResNet, ODENet, and variants

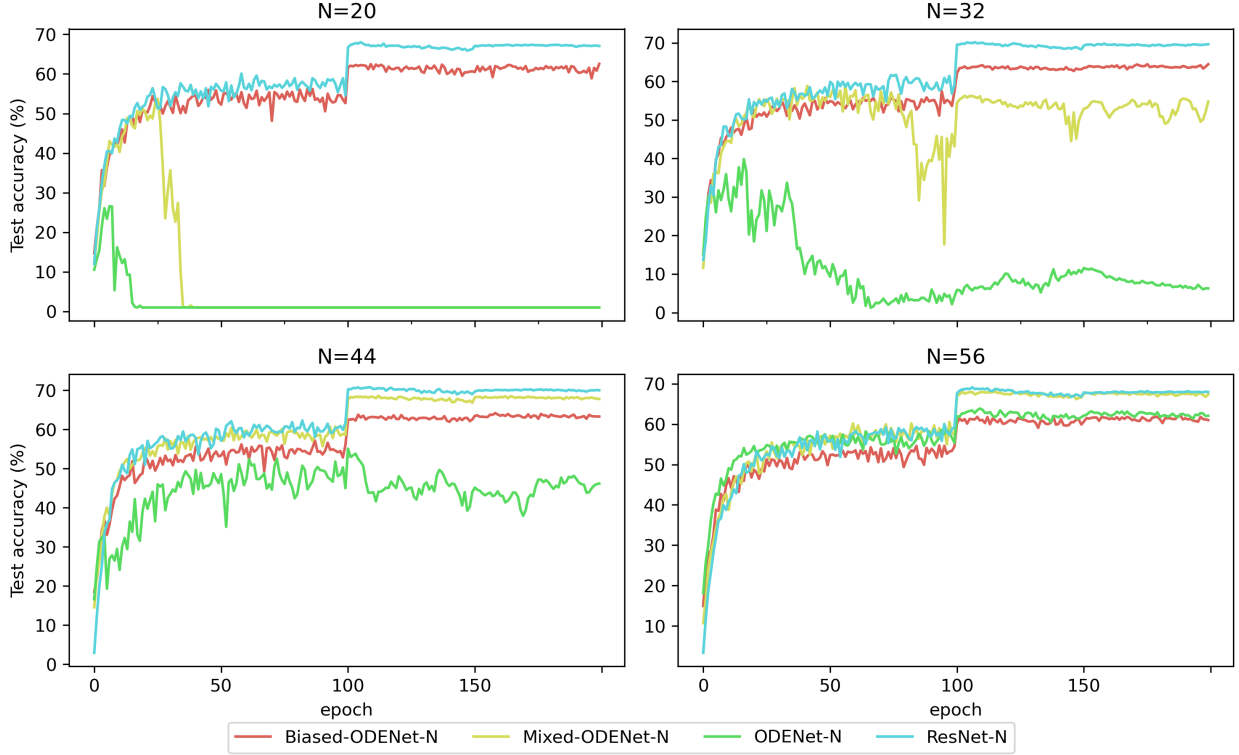
Model		Parameter size [MB]
<b>ResNet-N</b>	N=20	1.102288
	N=32	1.880016
	N=44	2.657744
	N=56	3.435472
<b>ODENet-N</b>	N=20	0.7028
	N=32	0.7028
	N=44	0.7028
	N=56	0.7028
<b>Mixed-ODENet-N</b>	N=20	0.81096
	N=32	0.996816
	N=44	1.182672
	N=56	1.368528
<b>Biased-ODENet-N</b>	N=20	0.625104
	N=32	0.625104
	N=44	0.625104
	N=56	0.625104

### 4.3 Accuracy

In this experiment, SGD [9] is used as an optimization function. As L2 regularization, regularization parameter  $1 \times 10^{-4}$  is added to each layer. For the training process, the number of epochs is 200. The learning rate is started with 0.01, and it is reduced by  $\frac{1}{10}$  when the epoch becomes 100 and 150.

Figure 5 shows the evaluation results of accuracy in the four network architectures listed in Table 2. As shown in the graphs, when N is small (e.g., N=20), the training results are unstable especially in **ODENet-N** and **Mixed-ODENet-N**. When N is large (e.g., N=56), all the architectures become stable and show a similar tendency. The results show that **ODENet-N** and its variants have similar properties to **ResNet-N**.

Below are observations of the four architectures.

Figure 5: Accuracy of four network architectures when  $N=\{20,32,44,56\}$ 

- In **Mixed-ODENet-N**, the accuracy is the almost same as **ResNet-N** when  $N$  is large (e.g.,  $N=44$  and  $56$ ). More specifically, accuracies of **ResNet-44** and **Mixed-ODENet-44** are 70.74% and 68.58%, and those of **ResNet-56** and **Mixed-ODENet-56** are 69.09% and 68.11%; thus there is up to 1.6% accuracy loss. The accuracy difference between **ResNet-44** and **ResNet-56** is 1.15%, while that of **Mixed-ODENet-44** and **Mixed-ODENet-56** is only 0.47%; thus, they are robust against overfitting (e.g., degradation of generalization ability) due to larger  $N$ .
- In **Biased-ODENet-N**, the accuracy is the second highest next to that of **ResNet-N** when  $N$  is small (e.g.,  $N=20$  and  $32$ ). Accuracies of **ResNet-20** and **Biased-ODENet-20** are 68.02% and 62.54%, and the accuracy difference is 5.48%. Those of **ResNet-32** and **Biased-ODENet-32** are 70.16% and 64.46%, and the difference is 5.70%. These differences are large compared to those of **Mixed-ODENet-N** when  $N$  is large (e.g.,  $N=44$  and  $56$ ). Still, **Biased-ODENet-N** is stable for all the sizes. The reason for this stable result is that it uses a single ODEBlock and the step size was small, and thus it could acquire the dynamics accurately. Since it is relatively stable, we can use **Biased-ODENet-N** even if the optimal network architecture is not known yet.
- In **ODENet-N**, the accuracy is the second highest next to that of **ResNet-N** when  $N$  is large (e.g.,  $N=44$  and  $56$ ). However, it is unstable when  $N$  is small. The reason for this instability is that the step size was small and thus it could not acquire the dynamics sufficiently. In **ODENet** and its variants, it is interpreted that connections of **ResNet** layers are continuous. It is pointed out that there may be a possibility that **ODENet** cannot compute the gradients accurately [10]. It might be one reason for the instability when  $N$  is small.

Among the three architectures implemented on the FPGA, **Mixed-ODENet-N** is the highest accuracy, followed by **ODENet-N** and **Biased-ODENet-N** when  $N$  is 56. This order is consistent with the parameter size; that is, the larger parameter size is higher accuracy. Please note that the accuracy highly depends on  $N$ . When  $N$  is small or optimal  $N$  is not known yet, **Biased-ODENet** is a practical choice. When  $N$  is large (e.g.,  $N=44$  or more), **Mixed-ODENet-N** is advantageous since its accuracy is high and it is robust against overfitting (e.g., degradation of generalization ability) due to larger  $N$ . **ODENet-N** has an intermediate property between **Biased-ODENet** and **Mixed-ODENet-N**.

Table 4: Execution time and speedup of four network architectures (CPU: Cortex-A9, FPGA: conv\_x16)

Model		CPU total [s]	CPU layer3_2 [s]	Ratio of layer3_2	FPGA layer3_2 [s]	FPGA total [s]	Overall speedup
<b>ResNet-N</b>	N=20	0.79	0.17	21.03%	—	—	—
	N=32	1.26	0.33	26.05%	—	—	—
	N=44	1.72	0.49	28.50%	—	—	—
	N=56	2.17	0.65	30.05%	—	—	—
<b>ODENet-N</b>	N=20	0.72	0.14	19.77%	0.03	0.59	1.21
	N=32	1.06	0.26	24.22%	0.07	0.85	1.25
	N=44	1.35	0.37	27.64%	0.10	1.05	1.28
	N=56	1.76	0.49	27.67%	0.13	1.38	1.27
<b>Mixed-ODENet-N</b>	N=20	0.77	0.14	18.67%	0.03	0.64	1.21
	N=32	1.20	0.26	21.60%	0.07	0.98	1.22
	N=44	1.61	0.37	23.13%	0.10	1.32	1.22
	N=56	2.03	0.49	24.03%	0.13	1.65	1.23
<b>Biased-ODENet-N</b>	N=20	0.68	0.37	54.51%	0.10	0.39	1.75
	N=32	1.03	0.72	69.72%	0.20	0.49	2.11
	N=44	1.37	1.06	77.50%	0.27	0.58	2.34
	N=56	1.71	1.40	81.82%	0.39	0.69	2.50

#### 4.4 Execution Time

ODENet and its variants implemented on the FPGA mentioned in Section 3 are evaluated in terms of prediction time. An image size in CIFAR-100 dataset is (channel, height, width) = (3, 32, 32), and prediction time for each image is measured. As an FPGA platform, TUL PYNQ-Z2 board (see Figure 4) that integrates PS and PL parts is used in this experiment. As listed in Table 1, in PS part, two ARM Cortex-A9 processors are running at 650MHz. In PL part, the operating frequency of the dedicated circuits is 100MHz. Vivado 2017.2 was used for the design synthesis and implementation of the ODEBlock of layer3\_2 implemented on PL part. We assume conv\_x16 implementation that uses 16 multiply-add units for the convolution and ReLU steps.

Table 4 shows the execution time and speedup rate when layer3\_2 of ODENet and its variants is executed on PL part and the others are executed on PS part of the FPGA board. PL part is not used in ResNet, so all the layers are executed on the PS part in the case of ResNet. Please note that data transfer overhead between PS and PL parts is not considered since it highly depends on the underlying platform.

- As shown in Table 4, execution time of layer3\_2 takes up 18.67% to 30.05% of total execution time except for **Biased-ODENet-N**. The ratio of layer3\_2 increases as N is increased.
- In **Biased-ODENet-N**, layer3\_2 is heavily used intentionally; thus, the ratio of layer3\_2 is quite high and increases fast compared to the other architectures. It is 2.50 times faster than a pure software execution when N is 56, which is the largest overall speedup by the FPGA.
- Regarding **ODENet-N** and **Mixed-ODENet-N**, the overall speedup by the FPGA for **ODENet-N** is higher than that of **Mixed-ODENet-N** in all the sizes. This is because the ratio of layer3\_2 in **ODENet-N** is slightly higher than that in **Mixed-ODENet-N** and the speedup rate of only layer3\_2 by the FPGA is almost constant.

In summary, the overall speedup rate by the FPGA is the highest in **Biased-ODENet-N**, followed by **ODENet-N** and **Mixed-ODENet-N**. This order is opposite to the parameter size (Section 4.2) and the maximum accuracy when N is 56 (Section 4.3). That is, the speedup rate becomes high when the parameter size is small, while the maximum accuracy is high when the parameter size is large enough; thus there is a tradeoff. Regarding the overall speedup compared to the original ResNet, **Biased-ODNet-56** is 3.17 times faster than a pure software execution of **ResNet-56**. Although the overall speedup by the FPGA is smallest in **Mixed-ODENet-20**, it is 1.24 times faster than a software execution of **ResNet-20**. Although only layer3\_2 is implemented on the programmable logic in our current implementation, the results show that it can sufficiently accelerate the prediction tasks compared to the original **ResNet-N**.

#### 4.5 FPGA Resource Utilization

Table 5 shows resource count and utilization of layer3\_2 implemented on PL part of the FPGA for ODENet and its variants in this paper. Here, we show the result when  $n$  multiply-add units are used for the convolution and ReLU steps denoted as conv\_xn implementation.



Table 5: Resource count and utilization of layer3\_2 on Zynq XC7Z020

	BRAM		DSP		LUT		FF	
conv_1	140	(100.00%)	8	(3.63%)	1692	(3.18%)	927	(0.87%)
conv_4	140	(100.00%)	20	(9.09%)	3048	(5.73%)	1411	(1.33%)
conv_8	140	(100.00%)	36	(16.36%)	4907	(9.22%)	2059	(1.94%)
conv_16	140	(100.00%)	68	(30.91%)	12720	(23.91%)	6378	(5.99%)
conv_32	140	(100.00%)	132	(60.00%)	23331	(43.86%)	10170	(9.56%)

As shown in the table, BRAM utilization is 100% and cannot implement more weight parameters or larger feature maps without relying on external DRAMs. A timing constraint of the FPGA board is 100MHz. Only conv\_x32 could not satisfy the timing constraint, so the execution time shown in Table 4 assumes the conv\_x16 implementation. In this case, the utilizations of DSP, LUT, and FF still have room; thus, we can implement some other application-specific logic on PL part of the FPGA.

## 5 Summary

In order to offload a part of ResNet building blocks to PL part of low-cost FPGA devices, **ODENet-N** in which a lot of building blocks are replaced with ODEBlock was implemented. As its variants, **Biased-ODENet-N** that heavily uses layer3\_2 implemented on PL part of the FPGA, and **Mixed-ODENet-N** in which only the last building block is replaced with ODEBlock were also proposed. They were evaluated using CIFAR-100 dataset.

- The evaluation results showed that parameter size of **Biased-ODENet-56** is the smallest and it can reduce parameters by 81.80% compared to **ResNet-56**.
- Regarding the accuracy, when N is large (e.g., N=44 and 56), **Mixed-ODENet-44** shows the highest accuracy among the ODENet and its variants. Actually, accuracy of **ResNet-44** is 70.74% while that of **Mixed-ODENet-44** is 68.58%; in this case, the accuracy loss is approximately 2%. When N is small (e.g., N=20 and 32), **Biased-ODENet-N** shows the best accuracy, though there is approximately 5% accuracy loss compared to **ResNet-N**.
- Regarding the overall speedup by the FPGA, **Biased-ODENet-N** is the fastest when layer3\_2 is parallelized by 16 multiply-add units on the PL part. When N is 56, it is 2.50 times faster than a software execution, and it is 3.17 times faster than **ResNet-56**.

In summary, **Biased-ODENet-N** is the best in terms of the parameter size and performance, followed by **ODENet-N** and **Mixed-ODENet-N**. However, the order is opposite with respect to the maximum achievable accuracy; thus there is a tradeoff. Please note that the accuracy depends highly on N. Actually, **Biased-ODENet-N** shows a better accuracy and performance when N is small. Our observation from the results is that **Biased-ODENet-N** is the best when N is less than or equal to 44 or speedup is the primary goal; on the other hand, **Mixed-ODENet-N** is the best when N is greater than or equal to 44 and accuracy is the primary requirement.

As a future work, we are working on the accuracy loss issue when the adjoint method is used for the training process. Further experiments using more accurate ODE solvers, such as Runge-Kutta method, are necessary. Lastly, we are planning to offload the training process of ODENets to FPGA devices.

## References

- [1] Kaiming He, Xiangyu Zhang, Shaoqing Ren, and Jian Sun. Deep Residual Learning for Image Recognition. In *Proceedings of the IEEE Conference on Computer Vision and Pattern Recognition (CVPR'16)*, pages 770–778, Jun 2016.
- [2] Ricky T. Q. Chen, Yulia Rubanova, Jesse Bettencourt, and David Duvenaud. Neural Ordinary Differential Equations. In *Proceedings of the Annual Conference on Neural Information Processing Systems (NeuroIPS'18)*, pages 6572–6583, Dec 2018.
- [3] Mineto Tsukada, Masaaki Kondo, and Hiroki Matsutani. A Neural Network-Based On-device Learning Anomaly Detector for Edge Devices. *IEEE Transactions on Computers*, 69(7):1027–1044, Jul 2020.
- [4] Sergey Ioffe and Christian Szegedy. Batch Normalization: Accelerating Deep Network Training by Reducing Internal Covariate Shift. In *Proceedings of the International Conference on Machine Learning (ICML'15)*, pages 448–456, Jul 2015.

- 
- [5] Vinod Nair and Geoffrey E Hinton. Rectified Linear Units Improve Restricted Boltzmann Machines. In *Proceedings of the International Conference on Machine Learning (ICML'10)*, pages 807–814, Jun 2010.
  - [6] William H. Press, Saul A. Teukolsky, William T. Vetterling, and Brian P. Flannery. *Numerical Recipes. The Art of Scientific Computing, 3rd Edition*. Cambridge University Press, 2007.
  - [7] L. S. Pontryagin, V. G. Boltyanskii, R. V. Gamkrelidze, and E. F. Mishechenko. *The Mathematical Theory of Optimal Processes*. John Wiley & Sons, 1962.
  - [8] PYNQ - Python Productivity for Zynq. <http://www.pynq.io/>.
  - [9] Ohad Shamir and Tong Zhang. Stochastic gradient descent for non-smooth optimization: Convergence results and optimal averaging schemes. In *Proceedings of the International Conference on Machine Learning (ICML'13)*, pages 71–79, Jun 2013.
  - [10] Amir Gholaminejad, Kurt Keutzer, and George Biros. ANODE: Unconditionally Accurate Memory-Efficient Gradients for Neural ODEs. In *Proceedings of the International Joint Conference on Artificial Intelligence (IJCAI'19)*, pages 730–736, Aug 2019.